

Effect of Lithium Intercalation on the Structure of Non-graphitizable Carbon: Small-Angle Neutron Scattering

S. M. MAMUN*, Takashi KAMIYAMA, Miki NAGAO¹, Kuniaki TATSUMI², Takashi TAKEDA²,
Michihiro FURUSAKA, Toshiya OTOMO, Susumu IKEDA, Tadaaki MATSUMURA¹ and
Ryoji KANNO¹

*Neutron Science Laboratory (KENS), Institute of Materials Structure Science,
High Energy Accelerator Research Organization (KEK), Tsukuba 305-0801, Japan*

¹*Department of Chemistry, Kobe University, Nada, Kobe, Hyogo, 657-8501, Japan*

²*Osaka National Research Institute, 1-8-1, Midorigaoka, Ikeda, 653-8577, Japan*

Recent developments in rechargeable Li-ion battery technology include the use of lithium-carbon compounds instead of metallic anodes. Non-graphitizable carbons offer high capacity as the anode material but its large irreversible capacity must be solved. The ultimate goals of the present work are to understand the origin of the high capacity and large irreversible capacity in conjunction with the structural change due to Li intercalation and thus to establish a scientific basis for optimizing their performance in real batteries. 'House of cards' model is considered and emphasis is given to find out the size of the pores present in the carbon fibers prepared from an isotropic petroleum pitch and heat treated at 1200°C. Small angle neutron scattering and wide angle neutron scattering results provide enlargement of pores and *d*-spacing of graphene layers after Li intercalation.

KEYWORDS: Li batteries, non-graphitizable carbon, Li intercalation, structure analysis, neutron scattering

§1. Introduction

Non-graphitizable carbons play a significant role in recent developments of rechargeable Li-ion batteries. They give higher capacity as anode materials than the capacity of LiC₆ (372 mAh·g⁻¹) with a significant performance in the potential range from 0 to 0.1 V (vs. Li/Li⁺). The capacity below 0.1 V looks like a plateau during charge and discharge and is very attractive for anodes of high energy-density batteries. The charge-discharge mechanism studied by ⁷Li-nuclear magnetic resonance (⁷Li-NMR) suggested two types of Li species during lithiation process; one type of Li is the same as those in graphitizable carbons, and the other is quite different.¹⁾ The former is thought to be in the inter-layer space between graphene layers, and the latter is Li clusters with metallic character, which causes a significant capacity below 0.1 V.²⁾ The structure information on the lithiation process is, however, still ambiguous, because weakly periodic structures of the carbon make it difficult to understand the structural changes during Li insertion and extraction by X-ray diffraction analysis. Small-angle X-ray scattering is not sensitive to voids present in the sample.³⁾ Neutron scattering technique is efficient to understand the structure of non-graphitizable carbons before and after Li intercalation. In the present study, the structures of the carbon and lithiated carbon were studied by small angle neutron scattering (SANS) to understand the structural changes during the lithiation process.

§2. Experimental

Carbon fiber prepared from an isotropic petroleum pitch (nominal diameter of 10 μm, FIP, Petoca), a precursor of non-graphitizable carbons, was heat-treated at 1200°C. Electrochemical Li insertion was performed in a three-electrode cell with 1 mol·dm⁻³ solution of LiClO₄ in a 50:50 (by volume) mixture of ethylene carbonate (EC) and diethylcarbonate (DEC) at 27°C. The reference and counter electrodes were Li metal. Carbons are lithiated with two different concentrations of Li and we call them partially lithiated carbon (LiC_{10.4}) and fully lithiated carbon (LiC₇). Both LiC_{10.4} and LiC₇ were prepared by galvanostatic reduction. The fully lithiated carbon was prepared by short circuiting the cells for 12 h after galvanostatic reduction (25 mA·g⁻¹) to 0 V. The neutron diffraction data were collected using a time of flight (TOF) diffractometer VEGA from three samples (carbon, LiC_{10.4} and LiC₇), and SANS experiments were carried out by a TOF diffractometer SWAN for the same samples, at the KENS pulsed spallation neutron source at High Energy Accelerator Research Organization (KEK).

§3. Results and Discussion

Figure 1 shows SANS data obtained from SWAN for carbon, LiC_{10.4} and LiC₇. In the range 0.02 Å⁻¹ < *Q* < 0.04 Å⁻¹ there exist a number of discontinuities at different intensity levels. Although the origin of the discontinuity is not clarified yet, it is likely that there exists large structure distribution. In the range 0.1 Å⁻¹ < *Q* < 1.2 Å⁻¹ the curve shows a very big shoulder with flat tail which is the result of scattering from the voids superimposed with constant backgrounds. We will dis-

* On study leave, Department of Applied Physics and Electronics, Dhaka University, Dhaka 1000, Bangladesh.

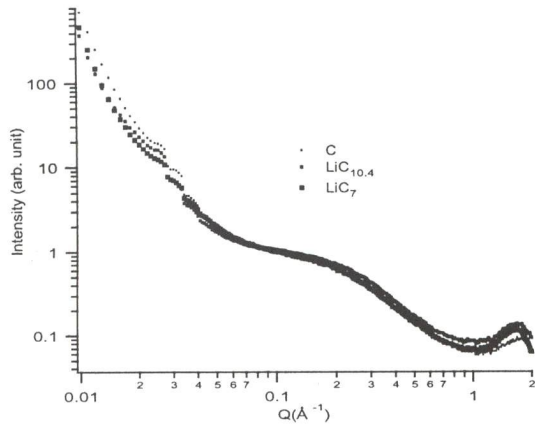


Fig. 1. SANS data for carbon, LiC_{10.4} and LiC₇; normalized to mass of carbon.

Table I. Fitting results: best-fit values obtained by eq. (3.1) for the scattering curves of carbon, LiC_{10.4}, and LiC₇.

Sample Name	$I(0)$ (arb. unit)	ξ (Å)	d_{002} (Å)
carbon	1.24	2.94	3.72
LiC _{10.4}	1.10	2.85	3.80
LiC ₇	1.12	3.19	3.87

cuss in detail about the void sizes later. In the range $1.2 \text{ \AA}^{-1} < Q < 2.0 \text{ \AA}^{-1}$ we observed the 002 Bragg reflection of graphene layers.

In the present work we focused on the shoulder and Bragg peak region to extract informations about void sizes and 002 plane spacings before and after Li intercalation. Data is fitted by the following equation:

$$I = A Q^{-4} + \frac{I(0)}{\{1 + (\xi Q)^2\}^2} + B e^{-\frac{(Q-Q_0)^2}{\sigma^2}} + B k g \quad (3.1)$$

On the right side of eq. (3.1), first term obeys Porod law. Tail part or the intensity at higher Q -region of big structure started decaying from 0.04 \AA and overlaps with the initial part of the scattering from voids at around 0.07 \AA .

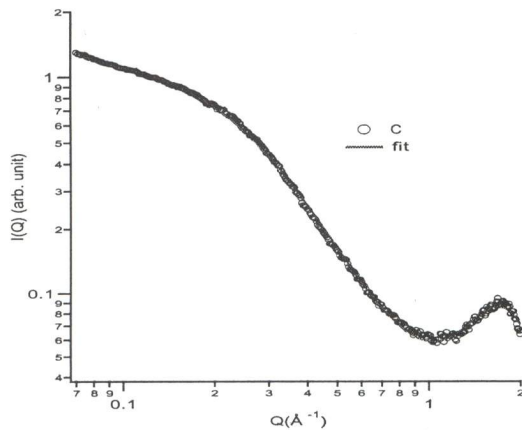


Fig. 2. SANS data and fitting curve for carbon.

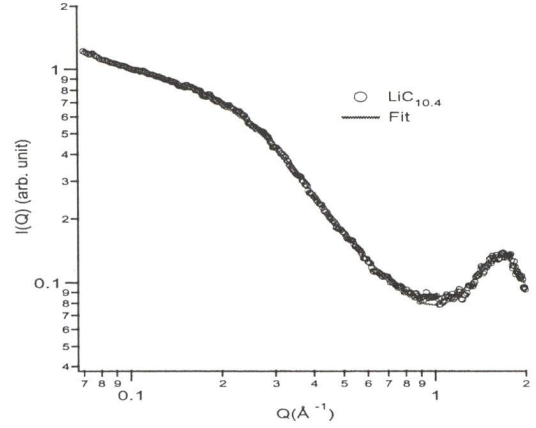


Fig. 3. SANS data and fitting curve for LiC_{10.4}.

According to porod law the tail part should be proportional to Q^{-4} . second term is Debye-Bueche function, third term is Gaussian function signifying Bragg contribution and the last term, Bkg , is for constant background. ξ is called correlation length which is related to the radius of gyration of the pores, Q_0 represents the position of the 002 Bragg peak produced by graphene layers, and $I(0)$ is the intensity extrapolated to $Q = 0$ in Debye-Bueche function and can be expressed as:

$$I(0) = n(\Delta\rho V_P)^2 \quad (3.2)$$

where n is the number density of pores, $\Delta\rho$ is the difference in scattering length density between matrix and pore, and V_P is the volume of pore.⁴⁾ In this work we haven't calculated n because absolute callibration of $I(0)$ is not done yet and in all figures intensity is plotted in arbitrary unit. For low Q region Debye-Bueche equation can be approximated as follows:

$$I = \frac{I(0)}{\{1 + (\xi Q)^2\}^2} = \frac{I(0)}{1 + 2\xi^2 Q^2 + \xi^4 Q^4} \approx \frac{I(0)}{1 + 2\xi^2 Q^2} \approx I(0)\{1 - 2\xi^2 Q^2\} \quad (3.3)$$

For low Q region Guinier equation can be approximated as follows:

$$I = I(0)e^{-\frac{R_g^2 Q^2}{3}} = I(0)\{1 - \frac{R_g^2 Q^2}{3} + \dots\} \approx I(0)\{1 - \frac{R_g^2}{3} Q^2\} \quad (3.4)$$

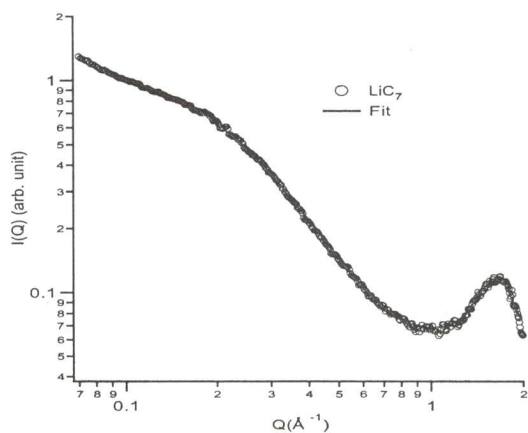
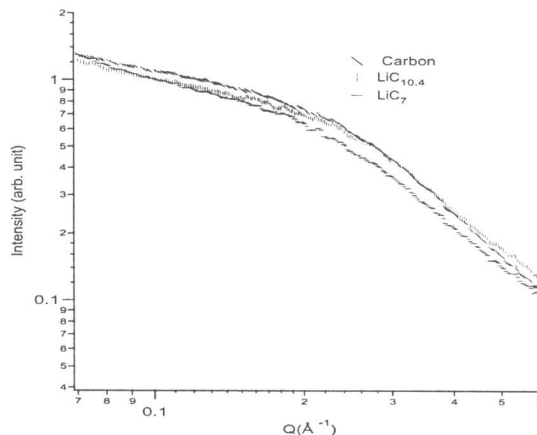
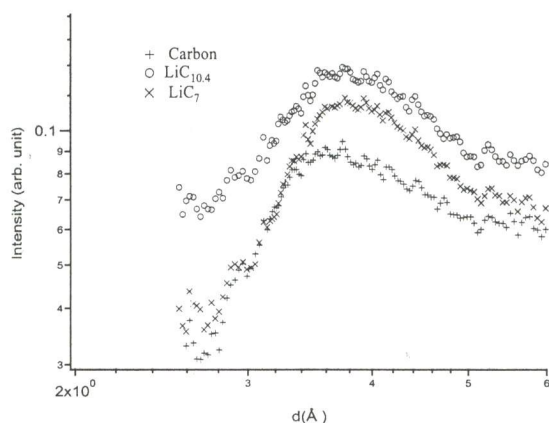
Where R_g is radius of gyration and $I(0)$ is the same as in eq. (3.1).

It is evident from eqs. 3.3 and 3.4 that Debye-Bueche and Guinier equations become identical at low Q regions and ξ and R_g can be related as

$$2\xi^2 = \frac{R_g^2}{3} \Rightarrow R_g = 2.45\xi \quad (3.5)$$

So from the value of ξ obtained from fitting result we can easily estimate the pore size.

Figures 2, 3 and 4 show the fittings for carbon, LiC_{10.4}

Fig. 4. SANS data and least squares fitting curve for LiC_7 .Fig. 6. SANS data; shoulder shifts towards low Q for LiC_7 .Fig. 5. SANS data obtained from SWAN; the 002 Bragg peaks for carbon, $\text{LiC}_{10.4}$ and LiC_7 .

and LiC_7 respectively. Fitting results are shown in Table I. Figure 5 shows the 002 Bragg peaks. Statistics of the data around Bragg peaks is not good for SWAN and d_{002} values in Table I is not considered highly accurate.

It is obvious from figure 5 that after partial lithiation distance between graphene layers increases and no significant change after fully lithiation. Neutron diffraction data obtained from VEGA were analyzed precisely to know the distance between graphene layers. Kanno *et al.*⁵⁾ fitted VEGA data by the graphite-2H model with a hexagonal structure that led to lattice parameters with $a = 2.4064(7)$ Å, $c = 6.985(11)$ Å; and $a = 2.4186(6)$ Å, $c = 7.074(9)$ Å for carbon and lithiated carbon respectively. No significant differences were found in the peak positions between the fully and partially lithiated samples. This indicates that during partial lithiation Li-ions intercalates into the spacings between graphene layers and the 002 interplaner distance increases. When more Li go into the sample they don't go into the graphene layers. They go somewhere else.

Figure 6 shows that the shoulder shifts towards low Q

for fully lithiated sample (LiC_7). But no significant shift for partially lithiated sample ($\text{LiC}_{10.4}$). In Table I the correlation length, ξ , is large after fully lithiation signifying increase in void size. With the help of equation (3.5) radius of gyration, R_g , of the voids for carbon, $\text{LiC}_{10.4}$ and for LiC_7 can be calculated as 7.2Å, 7.0Å and 7.8Å, respectively.

From these scenario one point is clear that during partial lithiation almost all of the Li-ions intercalate in between graphene layers. This causes enlargement in d_{002} spacing between graphene layers. If lithiation is still continued, almost all of the extra Li-ions go into the voids and almost no further increase in d_{002} spacing occurs.

§4. Conclusion

Small and wide angle neutron scattering techniques have been employed by SWAN and VEGA instruments at KEK to study the structure and porosity of non-graphitizable carbon anode materials for rechargeable Li-ion batteries. The totality of results tend to support the 'house of cards' model. During charge-discharge mechanism graphene layers experience expansion and contraction and this might be the cause of break down of graphene layer structure resulting in low cyclability of hard carbons as anode materials.

To improve cycle performance we need to produce hard carbons with larger layer spacing. This will also provide easy access of Li-ions into the layers resulting in large capacity.

Acknowledgement

One of the authors (S. M. M.) would like to express his gratitude to the Ministry of Education, Science, Sports and Culture, Japan for awarding scholarship.

- 1) K. Tatsumi *et al.*: J. Power Sources **81-82** (1999) 397.
- 2) K. Tatsumi *et al.*: Chem. Commun. (1997) 687.
- 3) Suzuya *et al.*: J. Materials Research **11** (1996) 1169.
- 4) Agnès Claye and J.E. Fischer: Electrochim. Acta **45** (1999) 107.
- 5) Kanno *et al.*: J. Power Sources, in press.